

THE ANALYSIS OF DISSIMILAR METAL WELD JOINT FOR FRACTURE MECHANICS EVALUATIONS

June-soo Park

Korea Power Engineering Co., Inc.
150 Deokjin-dong, Yuseong-gu, Daejeon
Republic of Korea 305-353
Phone: +82-42-868-4111
Fax: +82-42-863-4862
E-mail: js_park@kopec.co.kr

Ha-cheol Song

Korea Power Engineering Co., Inc.
150 Deokjin-dong, Yuseong-gu, Daejeon
Republic of Korea 305-353
Phone: +82-42-868-4115
Fax: +82-42-863-4862
E-mail: hacheol@kopec.co.kr

Ki-seok Yoon

Korea Power Engineering Co., Inc.
150 Deokjin-dong, Yuseong-gu, Daejeon
Republic of Korea 305-353
Phone: +82-42-868-4117
Fax: +82-42-863-4862
E-mail: ksyoon2@kopec.co.kr

Taek-sang Choi

Korea Power Engineering Co., Inc.
150 Deokjin-dong, Yuseong-gu, Daejeon
Republic of Korea 305-353
Phone: +82-42-868-4004
Fax: +82-42-863-4862
E-mail: tschoi@kopec.co.kr

ABSTRACT

This study is concerned with the stress analysis and fracture mechanics evaluation for a sub-critical crack in the dissimilar metal weld (DMW). The DMW considered herein is a transition joint of the ferritic nozzle to austenitic safe-end using the Inconel A 82/182 buttering and weld deposit. Weld residual stresses in the DMW nozzle are computed by non-linear thermal elasto-plastic analysis using the axisymmetric finite element (FE) model, for which temperature-dependent thermal and mechanical properties of the materials involved are considered. A stress relief in the as-welded nozzle by cold hydrostatic test is examined, and the operation pressure and thermal stresses are computed for normal service conditions. Computed residual and operation stresses are then mapped into a three-dimensional (3-D) domain by revolving the axisymmetric results, and linear elastic fracture mechanics (LEFM) parameters for a semi-elliptical surface crack in the combined stress state are evaluated using the finite element alternating method (FEAM). Results of and discussions on the stress analysis and fracture mechanics evaluations are presented. It is found that the effect of weld residual stresses on the crack-driving forces is dominant, as high as three times or more than the operation stresses.

Keywords: Weld residual stress, Stress corrosion cracking, Dissimilar metal weld, Alloy 82/182, Finite element alternating method (FEAM).

1. INTRODUCTION

Dissimilar metal welds between carbon steels and stainless steels are commonly used in nuclear piping systems. In order to analytically examine fracture behaviors of sub-critical cracks such as stress corrosion cracks (SCCs) or fatigue cracks found in the DMW component, one may have to determine the three-dimensional stress state in the welded component including the fabrication-induced residual stresses. In this paper, the ferritic nozzle-to-austenitic safe-end weld which is typically employed to connect the low-alloy steel main-loop piping

and austenitic-stainless steel branch piping in pressurized water reactors (PWRs) is considered as the DMW joint. Materials considered here for the DMW nozzle are the low-alloy steel nozzle (ASME SA-182 F1), austenitic stainless steel-clad (AWS EQ308L/309L), austenitic stainless steel safe-end (SA-182 F347), and nickel-base buttering and weld metals (Alloy 82/182).

From PWR operation experiences, the nickel-base Alloy 82/182/600 is known to be susceptible to Primary Water Stress Corrosion Crack (PWSCC) in a high tensile stress field, and the DMW components with Alloy 82/182 weld metal prone to fatigue problems under thermal cycling service conditions (Bamford, 2003). In order to demonstrate the structural integrity of flawed DMW components, it is crucial to predict with a reasonable accuracy the fracture mechanics parameters for cracks. For this, quantitative information of the state of stress in the subject component must be available, including the weld residual stresses and system operation stresses.

Thermal stresses are induced in the welded component during welding process by non-uniform thermal expansion and contraction of both the weld metal and adjoining base metals. Consequently, residual stresses remain after welding is completed. Thermal strains produced in the joining region are accompanied by material's plastic deformation, shrinkage and distortion: Major contributing factors are the temperature fields developed in weld joint, yield strengths of the materials involved, thermal properties such as the expansion coefficient and diffusivity. In this study, material thermal and mechanical behaviours in the nozzle to safe-end DMW joint are simulated to numerically predict the weld residual stresses by the thermal elasto-plastic FE modelling (Karlsson, 1986) and (Dong, 2002). A cold-hydrostatic test for the DMW nozzle after the completion of welding is also simulated to examine a relief of the as-welded residual stresses. In order to calculate the operating pressure and thermal stresses in the DMW nozzle, conventional linear elastic FE analyses are carried out.

After the stress analyses mentioned above are done, fracture mechanics evaluations of a surface crack inside the DMW nozzle are performed. For the linear elastic fracture mechanics parameter of the crack, the stress intensity factor (K) is calculated on the basis of results of the residual and operation stress analyses. Different methods are available to solve the fracture mechanics problems, including finite element and boundary element methods, singular/hybrid finite elements, finite element alternating method, and path-independent integral methods (Atluri, 1986) and (Atluri, 1989). Here, the finite element alternating method which is very efficient in the computational analysis is considered for evaluating K values of the surface crack. To implement the FEAM, a newly developed in-house computer code, GCS1 (General Crack Solver 1), is utilized (J.H. Park, 2004). The K values along the crack front in the DMW nozzle under given stress conditions are obtained by the code using the principle of superposition. Contributions to the crack driving force by the weld residual stresses, operation pressure and thermal stresses are examined.

2. STRESS ANALYSES

2.1 Weld Residual Stress

Non-linear thermal and mechanical analyses of the DMW nozzle are carried out using the general purpose finite element program, ABAQUS Version 6.4, together with a few user subroutines (Hibbit, Karlsson & Sorensen, 2003). An insignificant influence of thermal stresses on temperature fields in the work pieces during welding enables an uncoupled thermo-mechanical analysis. The decoupled analysis of weld mechanical behaviours requires the heat transfer calculation for welding process, as a prerequisite. A simplified axisymmetric FE model developed for the DMW nozzle is shown in Fig. 1.

For discretizing the finite element method (FEM) solution domains, isoparametric linear elements utilizing a trapezoidal numerical integration scheme are used: 2420 nodes and 2310 elements in total. Temperature-dependent thermal properties are considered, including the latent heat during melting and resolidification processes occurred during welding. The convective and radiative heat losses are considered for all surfaces except for the area covered with weld flux. Appropriate boundary conditions are considered exploiting the axisymmetry. A combination of volumetric and surface heat fluxes is applied as the weld heat input model based on the rate of arc energy. Approximately 50 weld passes are used for the production for V-groove weld, while for the simulation purpose here they are grouped into 18 layers of lumped weld passes. For each computation stage of weld layers, the Model Change option as provided by ABAQUS is utilized. Two types of simulation are considered in this study, i.e., two different weld sequences employed to gouge and reweld the weld root inside the nozzle. For the joint, the gas tungsten arc welding (GTAW) and the shielded metal arc welding (SMAW) are used, and typical welding parameters are given in Table 1.

Transient displacement and stress analyses are performed to predict weld residual stresses in the nozzle weld after the welding is completed. For decoupled mechanical analyses, transient temperature fields in the nozzle

which are determined in the previous thermal analyses are exactly applied as thermal loadings. The FE models developed for the weld thermal analysis with lumped weld passes are also used for the mechanical model. Materials subject to the welding cycle are postulated to behave as an elasto-plastic continuum which obeys the Prandtl-Reuss equation for an associated flow rule. Thus, the time-independent incremental plasticity theory is adopted, for which an isotropic hardening rule is considered. The von Mises yield criterion is used to define the onset of yielding, and the associated flow rule to define the plastic strain rate when the stress reaches the yield surface. The incremental plasticity formulation for temperature-dependent equations of thermal elasto-plasticity can be found elsewhere (Karlsson, 1986). Temperature-dependent mechanical properties for the materials are also considered: The molten weld metal is assumed to be in a stress-free state, being expressed by the stress-strain relation of material.

2.2 Stress Relief and Operation Stress

A cold-hydrostatic test of the DMW nozzle is also simulated to calculate a partial relief of the as-welded residual stresses by pressure overloading. The pressure loading step is applied subsequently to the weld mechanical analysis steps by the same FE model. A hydrostatic test pressure of 3125 psi at 70 °F is applied inside the nozzle which is in the as-welded state of residual stresses, and the state of pre-operation stresses in the nozzle is finally obtained for use in the fracture mechanics evaluation.

In order to calculate the pressure and thermal stresses in the nozzle under the normal system operation condition, conventional stress analyses are carried out. Computations of stresses are conducted using the same axisymmetric FE model as used for the weld mechanics analysis but assuming the linear elastic material properties. The operation stresses are calculated for the nozzle by applying the fluid pressure and temperature equal to 2235 psi and 650°F, respectively.

2.3 Analysis Results

As a result of the thermo-mechanical analyses above, preoperational residual stresses in the DMW nozzle are obtained after the cold hydrostatic test is completed. For two types of weld sequence the results are presented in Figs. 2 and 3: A standard type (denoted as dsw-me01b) is to reweld the weld root at the bottom of the groove inside the nozzle after depositing a full depth of the groove is completed; and an improved one (dsw-me01c) is to do after one-third depth of the groove is deposited and to deposit the remaining depth following the reweld. Residual stresses remained after the completion of the welding processes and cold hydrostatic-pressure test are partially presented in Fig. 2, which shows the variations of axial stresses across the nozzle thickness in term of distance from the edge of the nozzle. It is noted that residual stresses are tensile near the inner surface of the nozzle and their gradients are relatively high in the region of the weld (Sections 2, 3 & 4). The maximum stress at a level of 66.0 ksi is found on Section 2 near the inner surface. A self-equilibrium of the residual stresses in the nozzle axial direction is manifested on each of the stress sections.

In Fig. 3, weld residual stresses on the inner and outer surfaces of the DMW nozzle are presented for the two types of weld sequence: Two plots at the top in the figure show the residual stress distributions for the nozzle's inner surface in the axial and circumferential directions, and the bottom ones for the outer surface stresses. Stress peaks in the axial direction are found in both the nozzle safe-end and buttering weld layer (67.7 ksi and 72.9 ksi, respectively) in case of the standard sequence (dsw-me01b), while a peak stress of 90 ksi in case of the hoop stress is found in the weld root. The residual stresses on the nozzle outer surface are presented in the bottom plots of Fig. 3 where, contrarily to the inner surface stresses, the effects of stress improvement by changing the weld sequence are not significant, in case of the hoop stresses in particular. By changing the weld sequence, peak values of the residual tensile stress in the weld region are decreased by more than two times in case of the inner surface stresses: The stress improvements in the axial direction are profound in both the safe-end and buttered layer near the weld root, while the weld root region is improved in case of the circumferential stress. In all cases, stress jumps appear across the interfaces between the dissimilar metals, because of the elastic singularity of materials involved.

Results of the stress relief obtained for the DMW nozzle by the hydrostatic test are not presented in detail here because of the space limitation. However, it is noted that calculated values of the stress relief are as high as 5.0 ksi tensile and 10.0 ksi compressive (both in the circumferential direction), small compared to the levels of the as-weld residual stresses.

Differences in thermal and mechanical properties of the weld metal and adjacent base materials involved and a high degree of the structural constraint to the weld shrinkage in the DMW nozzle are deemed to be major causes of such high residual stresses. The Mises-equivalent stress contours though not presented here indicate a complicated plastic deformation in the weld region after it is cooled. In comparison with values of the yield strength of materials involved, magnitudes of weld residual stresses in the DMW nozzle are found significantly

high, which may cause sub-critical cracks (i.e., stress corrosion crack or fatigue crack) to initiate at an earlier stage of the component design life.

3. FRACTURE MECHANICS EVALUATION

3.1 Evaluation Method

Figure 4 shows a three-dimensional (3-D) FE model of the DMW nozzle using 20-noded brick-type elements (on the left), which is mapped from the axisymmetric 2-D model. The FEAM solution domain shown on the right side of the figure is defined for the fracture mechanics evaluation from the 3-D model on the left. Stress intensity factors (SIFs) as the LEFM parameter are obtained for a semi-elliptical surface crack inside the nozzle. It has been known that the addition of the fictitious crack mesh increases the accuracy in FEAM (Nikishkov, 2001). So, the crack mesh for a full elliptical crack is used in the analysis of a semi-elliptical crack, as shown in Fig. 4. A half of the mesh corresponds to the real crack, and the other half corresponds to the fictitious one.

A general FEAM process flow chart to calculate SIFs of a single or multiple cracks is depicted in Fig. 5, and the calculation steps are implemented by the in-house computer code GCS1 Version 1.01 (KOPEC, 2004). An axial semi-elliptical surface crack is assumed to be present on the inner wall of the nozzle and the location of the center of ellipse is assumed to exist in the weld root, a region susceptible to stress corrosion cracking. For the axial crack, the circumferential component of stress plays major roles in the crack growth. Let the circumferential component of the stress be $\sigma_{\theta}(r, z)$ on the $\theta=0$ plane in the nozzle without a crack. Then the mode I stress intensity factor (K_I) of an axial crack lying on the $\theta=0$ plane can be obtained as $-\sigma_{\theta}(r, z)$ is applied on the upper and lower crack surfaces as external loads.

When using the FEAM, the K solutions for a crack in the finite body are obtained as a superposition of two solutions; an FEM solution for a finite body without the crack and an analytical solution for an infinite body with the crack. Detailed descriptions on the method and numerical verification of the FEAM are given in the papers (Nikishkov, 2001) and (J.H. Park, 2004). Since a crack is not included in the 3-D FE model, it becomes very easy to prepare the model. And the remesh procedure is not necessary in the crack growth analysis. In the analytical solution of the FEAM, a crack is modeled as a continuous distribution of displacement discontinuities and an integral equation is formulated and solved by using the symmetric Galerkin method. A semi-elliptical surface crack is considered, where a represents the crack depth from the inner surface and $2c$ the crack length. In this analysis $c/a=2$ is assumed. The crack is divided into a number of crack elements. When an 8-noded element is used as a crack element, the stress singularity at the crack front can be expressed by shifting the midside nodes towards the crack front by one quarter of the side length of the crack element. The values of K_I are calculated from the displacement discontinuity values between the upper and lower crack surfaces near the crack front.

3.2 Evaluation Results

For the semi-elliptical surface crack ($c/a = 2$, $a = 0.125$ in) postulated to exist in the weld root of the DMW nozzle, the K_I values are obtained. The weld residual stresses as the preoperational state and the normal operational coolant pressure and temperature loadings (2250 psi at 570 °F) are applied to the FEAM model, respectively. The model is assumed to have the elastic constants of $E = 26,000$ ksi and $\nu = 0.29$. Figure 6 shows calculated K_I curves along the crack front in the field of the weld residual stresses, pressure and thermal stresses, respectively. In the figure, all of the K_I curves show their maximum values at the $\phi = 90^\circ$ position where the axial distance equals to zero: They are, $K_I = 14.7$ ksi in^{1/2} by the weld residual stresses; 2.82 ksi in^{1/2} by the normal operation temperature; 1.78 ksi in^{1/2} by the normal operation pressure; and the total value of 19.4 ksi in^{1/2}.

From the results above, it can be noted that the K_I generated by the weld residual stresses is much larger than those by the normal operation pressure and thermal stresses. By the presence of the weld residual stresses in the DMW nozzle, the crack driving force during the normal system operation increases by a factor of three or more depending on the location along the crack front. The unsymmetrical variation for K_I values along the front of the semi-elliptical crack in the nozzle is noticed and this is due probably to the complex stress fields in the region of the weld root, resulting from the effects of dissimilar metal combination and different material section properties. By applying the K values to an appropriate equation available for the material's crack growth model, the calculation of crack growth rates for the material is straightforward.

4. CONCLUSIONS

From the stress analysis and fracture mechanics evaluations for the DMW nozzle, significantly high values of the preoperational residual stresses exceeding the materials' yield strengths are shown in the weld region, predominantly over the operation stresses, and this can play an important role to initiate sub-critical surface cracks

in the nozzle. Differences in thermal and mechanical properties of the weld metal and adjacent base materials involved and a high degree of the structural constraint to the weld shrinkage are deemed to be major causes of such high residual stresses in the DMW. The SIFs generated in the DMW nozzle by the weld residual stresses are much larger than those by the normal operation pressure and thermal stresses, and by the presence of the weld residual stresses, the crack-driving force during the normal system operation increases by a factor of three or more depending on the location along the crack front. A proper control of the weld residual stresses in the DMW components at the fabrication stage or during service is crucial to managing the material degradation of the components. For the welded components in the complicated state of stress including the residual and operation stresses, fracture mechanics evaluations of sub-critical cracks can be efficiently and economically implemented by using the FEAM combined with the FEM.

REFERENCES

1. W.H. Bamford and J.F. Hall, (2003), A review of Alloy 600 cracking in operating nuclear plants: Historical experience and future trends. Proceedings of Conference on Vessel Head Penetration Inspection, Cracking and Repairs, pp.1-8.
2. L. Karlsson, (1986), Thermal stresses in welding. "Mechanics and Mathematical Method, Volume 1, Thermal Stress I," R.B. Hetnarski, ed., North-Holland, Amsterdam, pp. 299.
3. P. Dong and J.K. Hong, (2002), "Recommendations for Determining Residual Stresses in Fitness-for-Service Assessment." WRC Bulletin 476, Welding Research Council, Inc., New York.
4. S.N. Atluri, (1986), Energetic approaches and path independent integrals in fracture mechanics. "Computational Methods in Mechanics of Fracture," North-Holland, Amsterdam.
5. S.N. Atluri and T. Nishioka, (1986), On some recent advances in computational methods in the mechanics of fracture. Plenary Lecture, Advances in Fracture Research, Proceedings of the 7th International Conference on Fracture (ICF7). V.3, pp.1923-1969.
6. J.H. Park, S.Y. Park, M.W. Kim, J.S. Park and T.E. Jin, (2004), Development of a code for 2-D elasto-plastic fracture mechanics analyses using the finite element alternating method. Key Engineering Materials, v.270-273, pp.1159-1164.
7. Hibbit, Karlsson & Sorensen, Inc., (2003), "ABAQUS/Standard User's Manual, Version 6.4." Providence, RI.
8. G.P. Nikishkov, J.H. Park and S.N. Atluri, (2001), SGBEM-FEM alternating method for analyzing 3-D non-planar cracks and their growth in structural components. Computer Modeling in Engineering and Science, v.2, pp.401-422.
9. Korea Power Engineering Company, Inc. (KOPEC), (2004), "General Crack Solver 1 User's Manual, Version 1.01." Daejeon, Republic of Korea.

Table 1. Welding process parameters used for the nozzle-to-safe end joint

Process	Current (A)	Voltage (V)	Welding rod diameter (mm)	Welding speed (mm/min, ave.)	Remark
GTAW	100-180	12-17	φ 2.4	90	Root weld only
SMAW	80-110	20-28	φ 3.2	120	

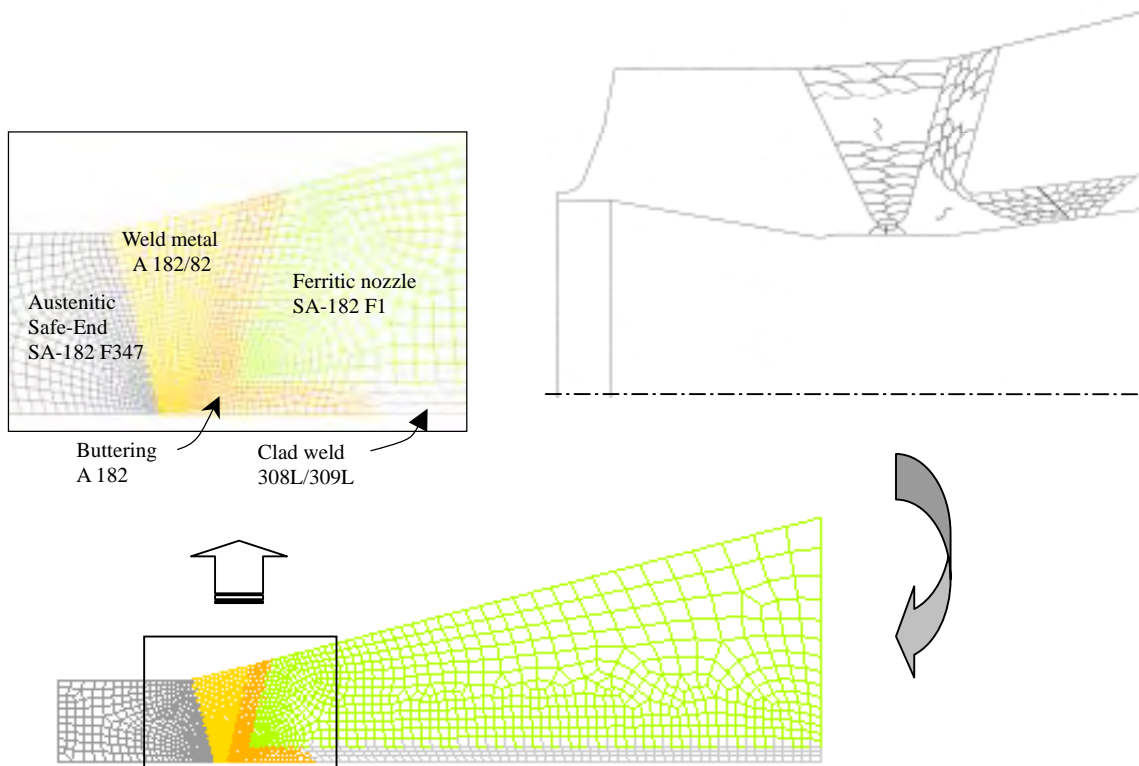


Figure 1. An axisymmetric FE model of the dissimilar metal weld nozzle developed for the stress analysis and fracture mechanics evaluation

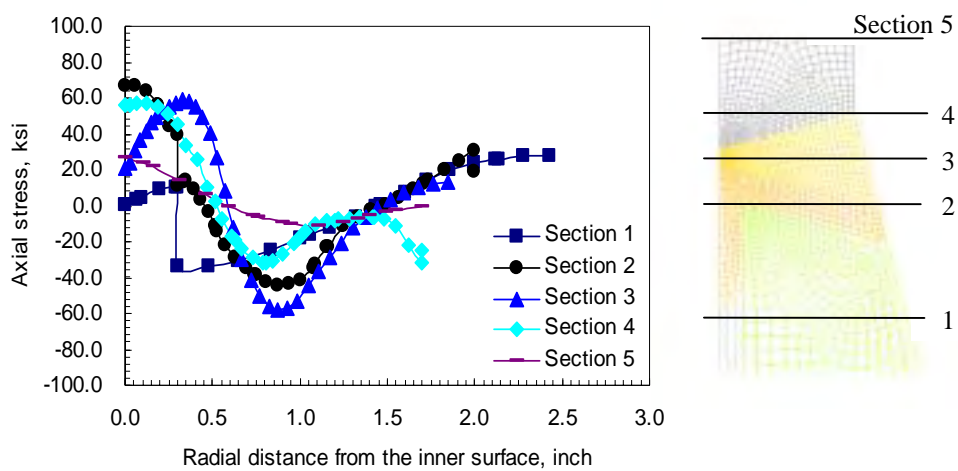


Figure 2. Distributions of weld residual stresses in the axial direction of the DMW nozzle after the welding processes and cold hydrostatic-pressure test are completed

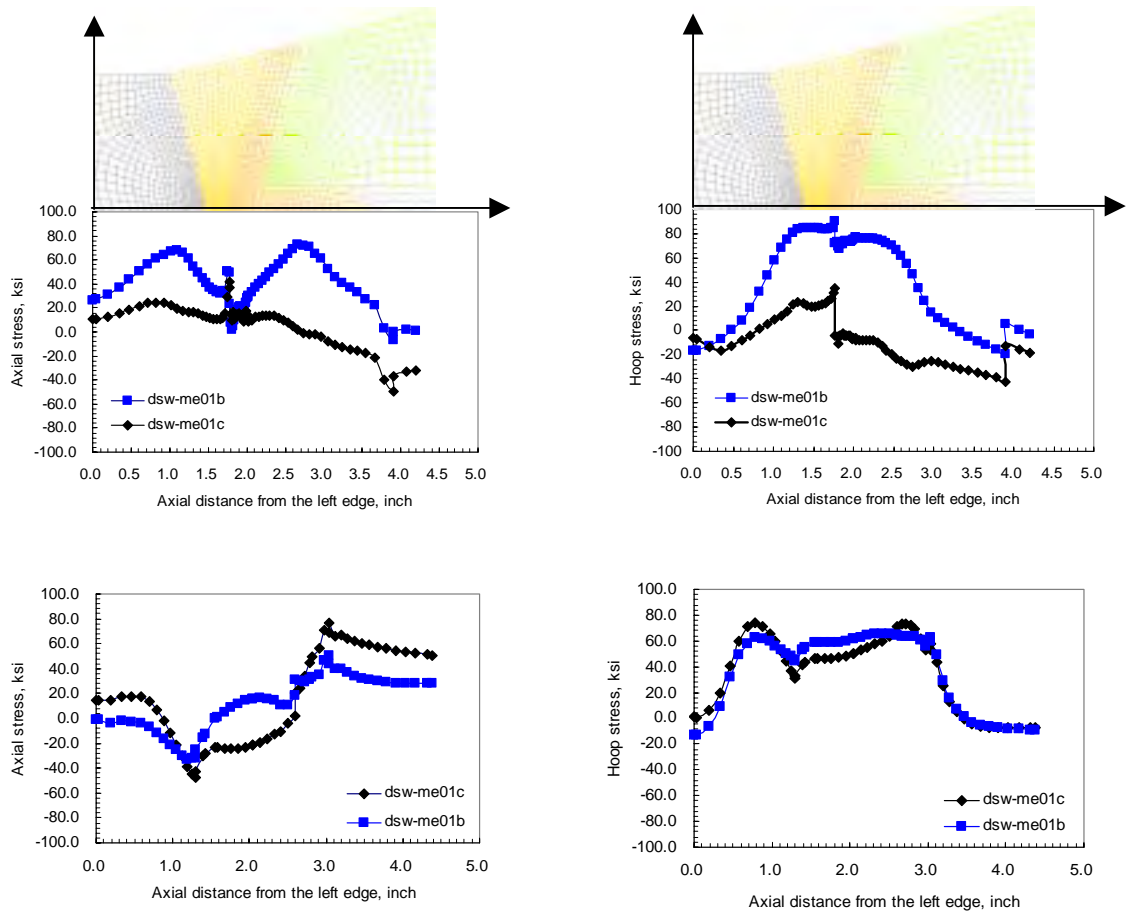


Figure 3. Weld residual stresses in the DMW nozzle in the axial and circumferential directions for two types of weld simulation (dsw-me01c and dsw-me01b); the nozzle inner surface stress (top) and the outer surface stress (bottom)

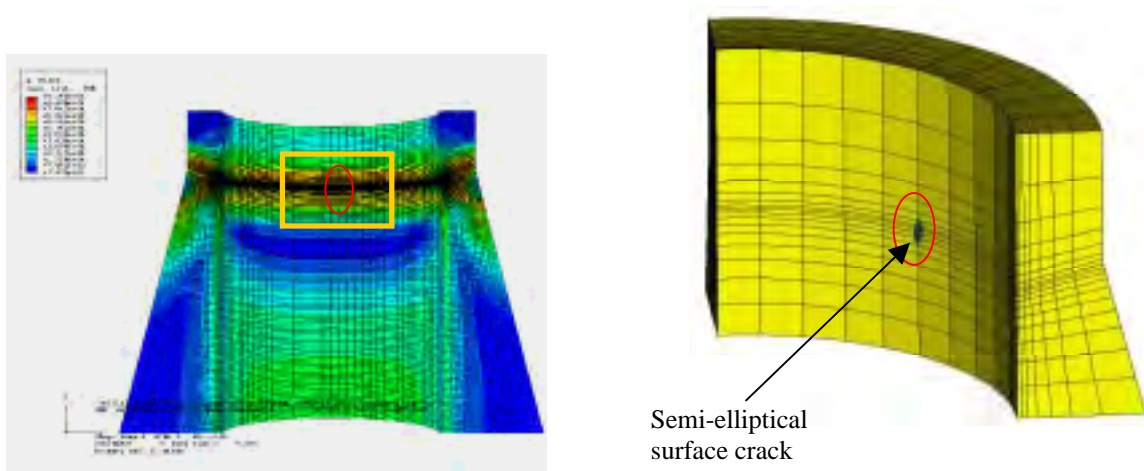


Figure 4. A 3-D FE model of the DMW nozzle (left) with the stress tensors mapped from the axisymmetric model and the 3-D FEAM model defined to calculate stress intensity factors for a semi-elliptical surface crack in the weld root inside the nozzle (right)

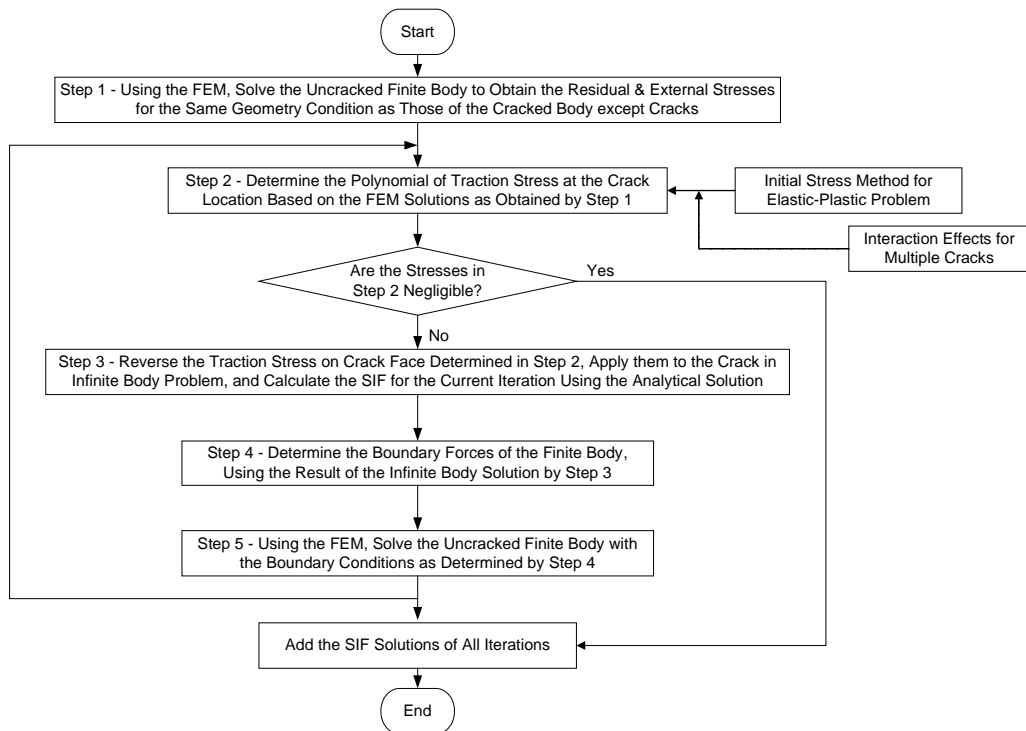


Figure 5. A general FEAM flow chart to determine stress intensity factors of crack(s) in the finite body using the analytical solution(s) for the infinite body

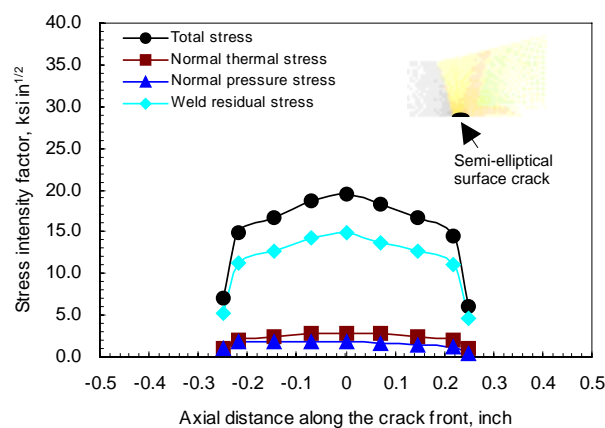


Figure 6. The mode I stress intensity factors (KI) along the crack front determined by the FEAM for the semi-elliptical surface crack ($c/a = 2$) located on the weld root inside the DMW n077le